Elsevier Editorial System(tm) for Plant Science
Manuscript Draft

Manuscript Number: PSL-D-13-00454R1

Title: Expression and localisation of a senescence-associated KDEL-cysteine protease from Lilium longiflorum tepals

Article Type: Full Length Article

Keywords: cysteine proteases, endoplasmic reticulum, Lilium, petal senescence, subcellular localisation, vacuole

Corresponding Author: Dr. Hilary Joan Rogers, PhD

Corresponding Author's Institution: Cardiff University

First Author: Riccardo Battelli

Order of Authors: Riccardo Battelli; Lara Lombardi; Piero Picciarelli; Roberto Lorenzi; Lorenzo Frigerio; Hilary Joan Rogers, PhD

Abstract: Senescence is a tightly regulated process and both compartmentalisation and regulated activation of degradative enzymes is critical to avoiding premature cellular destruction. Proteolysis is a key process in senescent tissues, linked to disassembly of cellular contents and nutrient remobilisation. Cysteine proteases are responsible for most proteolytic activity in senescent petals, encoded by a gene family comprising both senescence-specific and senescence up-regulated genes. KDEL cysteine proteases are present in senescent petals of several species. Isoforms from endosperm tissue localise to ricinosomes: cytosol acidification following vacuole rupture results in ricinosome rupture and activation of the KDEL proteases from an inactive proform. Here data show that a Lilium longiflorum KDEL protease gene, (LlCYP), is transcriptionally up-regulated, and a KDEL cysteine protease antibody reveals post-translational processing in senescent petals. Plants over-expressing LlCYP lacking the KDEL sequence show reduced growth and early senescence. Immunogold staining and confocal analyses indicate that in young tissues the protein is retained in the ER, while during floral senescence it is localised to the vacuole. Our data therefore suggest that the vacuole may be the site of action for at least this KDEL cysteine protease during tepal senescence.

Expression and localisation of a senescence-associated KDEL-cysteine protease from *Lilium longiflorum* tepals

Riccardo Battelli[a], Lara Lombardi[b], Piero Picciarelli[a], Roberto Lorenzi[b], Lorenzo Frigerio[c], Hilary J Rogers[d]

[a] Department of Crop Plant Biology, University of Pisa, Via Mariscoglio 34, 56124 (Italy)

[b] Department of Biology, University of Pisa, Via Ghini 5, 56126 Pisa (Italy)

[c] School of Life Sciences, University of Warwick, Coventry CV4 7AL, UK

[d] Cardiff School of Biosciences, Main Building, Cardiff University, PO Box 915, Cardiff CF10 3TL, UK

email addresses:

Riccardo Battelli riccardobattelli@gmail.com
Lara Lombardi llombardi@biologia.unipi.it
Piero Picciarelli picciarelli@agr.unipi.it
Roberto Lorenzi rlorenzi@biologia.unipi.it
Lorenzo Frigerio L.Frigerio@warwick.ac.uk
Hilary Rogers rogershj@cf.ac.uk

Corresponding author:

Hilary Rogers
School of Biosciences, Main Building, Cardiff University
Cardiff CF10 3TL
Tel: +44 (0)2920876352; Fax: +44 (0)2920874305
E-mail: rogershj@cf.ac.uk

Abstract

Senescence is a tightly regulated process and both compartmentalisation and regulated activation of degradative enzymes is critical to avoiding premature cellular destruction. Proteolysis is a key process in senescent tissues, linked to disassembly of cellular contents and nutrient remobilisation. Cysteine proteases are responsible for most proteolytic activity in senescent petals, encoded by a gene family comprising both senescence-specific and senescence up-regulated genes. KDEL cysteine proteases are present in senescent petals of several species. Isoforms from endosperm tissue localise to ricinosomes: cytosol acidification following vacuole rupture results in ricinosome rupture and activation of the KDEL proteases from an inactive proform. Here data show that a *Lilium longiflorum* KDEL protease gene, (*LlCYP*), is transcriptionally up-regulated, and a KDEL cysteine protease antibody reveals post-translational processing in senescent petals. Plants over-expressing *LlCYP* lacking the KDEL sequence show reduced growth and early senescence. Immunogold staining and confocal analyses indicate that in young tissues the protein is retained in the ER, while during floral senescence it is localised to the vacuole. Our data therefore suggest that the vacuole may be the site of action for at least this KDEL cysteine protease during tepal senescence.

188 words

Key words: cysteine proteases, endoplasmic reticulum, *Lilium*, petal senescence, subcellular localisation, vacuole.

1. Introduction

Petal senescence is a tightly regulated process involving, in most species, nutrient remobilisation and terminating in cell death. In many species this is accompanied by organ abscission [1,2]. In some species this process is coordinated by the growth regulator ethylene, while in others, including lilies, ethylene does not appear to play a major role in petal senescence [2]. At a cellular level, petal cell death is found to resemble most closely an autophagic pattern [3]. In several species, vesicles accumulate in the cytosol followed by enlargement of the central vacuole and ultimately vacuolar rupture (e.g. *Dianthus* [4], *Iris* [5], *Lilium longiflorum* [6]).

Nutrient remobilisation from senescent organs such as leaves and petals requires the action of a suite of degradative enzymes including nucleases, lipases, and proteases [1,2]. The synthesis and activation of these enzymes needs to be under tight temporal and spatial control to ensure the ordered breakdown of cellular macromolecules. Total protease activity generally increases with petal senescence while protein content falls (e.g. in *Alstroemeria* [7], *Hemerocallis* [8], *Sandersonia* [9]) and the pH optimum of protease activity in senescent petals is often relatively acidic (e.g. pH 5.5-6 in *Lilium longiflorum*, [6]). This suggests that these enzymes are either active in an acidic sub-cellular compartment such as the vacuole, or that they are activated in an acidified cytosol following vacuole rupture.

Transcriptomic studies have revealed the expression of genes encoding both cysteine proteases (EC 3.4.22), and aspartic proteases (EC 3.4.23) during floral senescence [5,10,11]. However using inhibitors for specific protease classes, it was shown that cysteine proteases are those primarily responsible for protease activity in senescent petals [7,9,12]. Cysteine proteases comprise a large gene family divided into several classes but those associated with senescence are mainly of the papain class [13]. In petals, multiple cysteine protease genes are expressed with varying temporal patterns [9,12,14]. For example in petunia only four out of nine cysteine protease genes expressed in petals were up-regulated in the later stages of petal senescence, three were down-regulated, two peaked in expression in early senescence after which their expression fell, and of the nine genes, expression of only one was senescence specific [12].

KDEL cysteine proteases form an important group of papain class cysteine proteases that are unique to plants and characterised by a C-terminal KDEL sequence that directs retention in the endoplasmic reticulum (ER) [13,15]. These proteases were initially identified in association with PCD in the castor bean (*Ricinus communis*) endosperm [16]. However they are also found in senescing petals of several species including *Hemerocallis* [17], *Sandersonia aurantica* [9] and *Dendrobium* [18]. Although the *in vivo* substrates of PCD-associated KDEL proteases are unknown, Helm *et al.* [15] showed that the castor bean enzyme has activity against some types of extensin proteins.

The castor bean KDEL cysteine protease was located to ricinosomes [16]. Ricinosomes are small organelles, first discovered in the castor bean endosperm [19,20], that derive from the ER [21]. They have subsequently also been found during castor bean nucellar programmed cell death (PCD; [22]), in tomato anthers, associated with anther dehiscence [23], and in senescent *Hemerocallis* petal cells [17]. A 45 kDa KDEL cysteine protease was localised to ricinosomes in *Hemerocallis* petal cells, however was not further investigated. During castor bean endosperm PCD, the ricinosomes appear at the same time as other PCD markers and then rupture, releasing their protease cargo into the cytosol. This is accompanied by autocatalytic processing of the KDEL protease from a 45 KDa to a 35 KDa mature form [16,21]. Acidification of isolated ricinosomes also results in KDEL protease processing and activation [21] supporting the hypothesis that cytosol acidification triggers ricinosome rupture and KDEL protein maturation. Thus it would seem that ricinosomes are distinct from autophagic-type vesicles that deliver their cargo to the vacuole prior to tonoplast rupture [1]. However, in *Vigna mungo* seeds, the SH-EP KDEL protease is transported to the vacuole via KDEL vesicles (KV) independently of the Golgi [24] a process dependent on the C-terminal KDEL sequence. In fact if the KDEL sequence is removed and the SH-EP protein over-expressed in transgenic Arabidopsis, the SH-EPΔKDEL is secreted into the extracellular spaces and plants die prematurely.

Lilium longiflorum is an important commercial cut flower with a well-characterised senescence programme [6] making it a useful model for studying mechanisms of floral senescence and PCD in an ethylene-insensitive species. Here data are presented on a *L. longiflorum* KDEL cysteine protease whose expression is strongly up-regulated during petal senescence. RFP fusions confirm it is translocated into the ER, however

immunogold staining indicates localisation of this protease to the vacuole rather than to ricinosomes during floral senescence. This is important in the context of understanding the role for KDEL cysteine proteases during petal senescence. Although a number of these proteins have been studied in different species [7,9,17,18] and are clearly highly expressed during the later stages of petal senescence, their mechanism of action in relation to the timing of cell death events remains uncertain. Here evidence is provided for localisation of these enzymes to the vacuole prior to tonoplast rupture.

2. Materials and methods

2.1. Plant material

Plant material was as described in [6]. *Lilium longiflorum* cv. "White Heaven" was grown in a commercial greenhouse and individual flowers harvested by cutting above the last leaf. Flowers were placed in distilled water and kept in a growth chamber at 22°C and 50% relative humidity. Flowers were harvested at stage D-2 (closed bud) and, under the conditions used, flower development and senescence progressed uniformly from stage D0 (loose bud, tepal tips beginning to separate, dehiscence begins, used as a reference stage) to stage D10 (full senescence, 10 days after the reference stage [6]. At D2 flowers were fully open, D3 is full bloom, at D4 first signs of senescence were visible (tepal translucence) which was more marked at D5. By D7 tepals were wilting and browning and by D10 the corolla had completely collapsed (though it does not abscise in this species).

2.2. RNA extraction and cDNA preparation

RNA was extracted with TRI reagent (Sigma, St Louis, MO, USA) according to the manufacturer's instructions. RNA was subjected to DNase treatment using a TURBO DNA-free kit (Ambion Inc., Austin, TX, USA) to remove contaminating genomic DNA. Five micrograms of RNA was reverse transcribed into cDNA using a High Capacity cDNA Reverse Transcription Kit (Applied Biosystems, Foster City, CA, USA) in accordance with the manufacturer's instructions.

2.3. Primer design

All the primers used in this work are listed in Supplementary Table I. For isolation of the *LlCYP* gene, degenerate primers CYPF and CYPR were designed from a

comparison of conserved regions of senescence-associated cysteine proteases from monocotyledonous species in the GenBank database [7]. Primers for 18s rRNA (PUV1, PUV2) were also designed by comparison of ribosomal genes from available monocotyledonous species [25].

2.4. Cloning of LlCYP

A 340bp fragment of a *Lilium longiflorum* KDEL protease gene was isolated from D4 outer tepal cDNA using degenerate primers CYPF and CYPR. The full-length cDNA was obtained using the BD SMART™ RACE cDNA Amplification Kit (BD Biosciences Clontech, Palo Alto, CA) using gene specific primers GSPF and GSPR. The whole ORF was amplified from D4 cDNA using primers LlCYPclF and LlCYPclR containing the BamHI and NotI restriction sites respectively and inserted into the pET21b vector (Novagen, Darmstadt, Germany). Clones were sequenced and compared with database sequences using the BLAST program (National Center for Biotechnology Information, NCBI). The ORF sequence was deposited in Genbank under accession number HF968474. DNA sequences were analysed using Bioedit (v. 7.0.5.3 [26] and a phylogenetic tree was produced using MEGA4 [27]; SignalP and TargetP [28] were used to analyse the sequence for a signal sequence.

2.5. Real-time qPCR

Primers with optimal characteristics in relation to secondary structure, self-hybridisation, GC content (40-60%), Tm (55-70 ^{o}C) and amplicon length (90-130 bp) (LlCypF and LlCypR) were designed with Primer3 software [29]. qPCR was carried out in a 7300 real-time PCR system (Applied Biosystems) using 50 ng of cDNA and SYBR® green PCR master mix (Applied Biosystems). The thermal profile was: 95°C x 2 min, followed by 40 cycles of 95°C x 15 sec, 64°C x 1 min. Expression of the ribosomal 18S gene, used for internal normalization, was analysed with PUV1 and PUV2 primers which amplify a 226 bp fragment. The thermal profile for 18S amplification was: 95°C x 2 min, followed by 40 cycles of 95°C x 15 sec, 55°C x 30 sec, 72°C x 30 sec. The PCR products were further analysed by a dissociation curve program (95 °C x 15 sec, 60°C x 1 min and 95°C x 15 sec) and all the reactions gave a single peak.

Data were analysed using the $2^{-\Delta\Delta_{CT}}$ method [30] and are presented as relative level of gene expression. All real-time qPCR reactions were run in triplicate with different cDNAs synthesized from three biological replicates.

194

195 *2.6. Heterologous expression of LlCYP gene in E. coli*

196 For heterologous expression of *LlCYP* gene, an overnight culture of *E. coli* BL21
197 carrying the *LlCYP* construct in the pET21b vector was used to inoculate 100 ml of LB
198 medium to an OD_{600} of 0.05-0.1. The culture was incubated at 37°C 200 rpm until an
199 OD_{600} of 0.4 had been reached. Expression was then induced by adding IPTG (Sigma)
200 to a final concentration of 0.5 mM and incubating overnight at 22°C. After collecting
201 the cells by centrifugation at 6000xg 10 min at 4°C, the pellet was resuspended in 2 mL
202 lysis buffer. Lysozyme was added to a final concentration of 1 mg/ml and the solution
203 was incubated on ice for 1 hour. After sonication for three times 30 s at 10 mÅ, samples
204 were transferred to Eppendorf tubes and centrifuged for 30 min at 13000 rpm, 4°C. The
205 supernatant was used for western blotting.

206

207 *2.7. Protein extraction and western blotting*

208 Frozen tepal tissue was ground in extraction buffer (50 mM Tris-HCl pH 7.5, 75 mM
209 NaCl 15 mM EGTA, 15 mM $MgCl_2$, 60 mM β-glycerophosphate) supplemented with
210 complete mini protease inhibitor cocktail (1 tablet per 10 ml; Roche Diagnostics
211 Corporation, Indianapolis, IN, USA). The suspension was sonicated for 30 sec at 10 µA
212 then centrifuged at 14000 xg at 4°C for 30 min. Protein content was quantified by the
213 Bradford method (Protein Assay Kit, Bio-Rad Laboratories, Hercules, CA) using a BSA
214 standard curve.

215 Equivalent amounts of protein (20 µg) were size-fractionated by SDS–PAGE on 12%
216 acrylamide gels. After electroblotting onto a Hybond-P PVDF membrane (Amersham
217 Pharmacia Biotech, Piscataway, NJ, USA), blots were blocked with 20 mM Tris-HCl
218 pH 7.5, 150 mM NaCl, 0.05% Tween 20 and 5% dry milk powder. Blots were then
219 incubated with polyclonal primary antibody raised against purified SlCysEP [23],
220 diluted 1:1000 in blocking solution, for 1 h, and washed twice in 20 mM Tris-HCl pH
221 7.5, 150 mM NaCl, 0.05% Tween 20 and 1% triton X-100. Blots were then incubated
222 with goat anti-rabbit secondary antibodies (Bio-Rad) diluted to 1:2500. To visualize
223 immunoreactive proteins, ECL Plus western-blotting detection reagent (Amersham
224 Biosciences) was used as substrate for the secondary antibody, following the
225 manufacturer's instructions.

226

227 *2.8. Immunogold labelling*

Outer tepals from flowers at stage D0, D3 and D5 were sampled and cut into 1 mm sections with a scalpel. Samples were fixed in 3% (v/v) formaldehyde, 3% (v/v) glutaraldehyde in 0.1 M phosphate buffer, pH 7.4, and post-fixed in 2% (w/v) OsO_4. Samples were dehydrated in an ethanol series at 4°C and infiltrated in LR White resin (Agar Scientific Ltd., Stansted, UK). For immunogold labelling, 100 nm thick sections were cut using a diamond knife, collected on 200 mesh nickel grids placed on drops of double-distilled water and incubated for 15 min in 5% (w/v) $NaIO_4$ followed by thorough washing in distilled water. Grids were then incubated for 5 min in 0.1 N HCl and washed again. Blocking was performed in 0.5% (w/v) BSA, 0.05% (v/v) Tween 20 and 0.05% (v/v) glycine in phospate buffer pH 7.4 for 10 min. Grids were incubated overnight with affinity-purified rabbit-anti SlCysEP IgG (28 mg mL^{-1}; [23]). After washing, the grids were incubated for 2 h at room temperature with secondary antibody, 10 nm colloidal gold-conjugated goat anti-rabbit IgG (Biocell Co. Ltd. Cardiff, UK), diluted 1:100 in blocking solution. The grids were washed in PBS 3 x 1 min and fixed for 3 min in 2% (v/v) glutaraldehyde in phospate buffer pH 7.4. Grids were then rinsed in distilled water, stained with 2% (w/v) uranyl acetate and Reynold's lead citrate [31] before being examined using a Philips EM 208 electron microscope at 80 KV accelerating voltage. Control grids were treated identically using pre-immune rabbit antiserum instead of primary antibody.

2.9. Preparation of RFP constructs

Two different expression vectors carrying RFP (red fluorescent protein)-tagged CYP protein under the control of the CaMV 35S promoter were made by using the Gateway site-specific recombinational cloning protocol (Invitrogen). The plasmid sp-RFP-AFVY [32] and the full-length *LlCYP* in pET21 were used as templates to amplify the RFP open reading frame and the different regions of the CYP sequence, respectively. All primers are listed in Supplementary Table 1.

For the amplicon sppro::RFP::CYP, primer 1 and 5 were used on the *LlCYP* sequence and primers 6 and 10 used on RFP sequence. Then the amplified RFP and CYP sequences were spliced together by fusion PCR using primer 1 in combination with primer 10**.** The product of this fusion was then used as a template together with the product of amplification of the *LlCYP* sequence with primers 8 and 9; the two templates were spliced together using primers 1 and 9.

For the amplicon sppro::RFP::CYPΔKDEL primer 1 and 5 were used on the *LlCYP* sequence and primers 6 and 10 used on the RFP sequence. Then the amplified RFP and

CYP sequences were spliced together by fusion PCR using primers 1 and 10**.** The product of this fusion was then used as template together with the product of amplification of the *LlCYP* sequence with primers 8 and 11; the two templates were spliced together using primers 1 and 11.

A high fidelity Taq polymerase was used (Phusion, Finnzyme) for all the PCRs above, and conditions were as follows: 95 ºC for 5 min; 32 cycles of 95 ºC 40 sec, 55 ºC 40 sec, 72 ºC 2.5 min, then 72 ºC for 10 min. The resulting amplicons (Supplementary Fig. 1) were sequenced, cloned into the pENTR/D-TOPO vector and transferred by recombination to the binary Gateway destination vector pK7WG2 (Invitrogen) under the control of the CaMV 35S promoter, following the manufacturer's instructions. The resulting constructs 35S::sppro::RFP::CYP (C3) and 35S::sppro::RFP::CYPΔKDEL (C4) were introduced into the *Agrobacterium tumefaciens* strain GV3101 and used for agroinfiltration, and for Arabidopsis stable transformation by floral dipping [33] followed by kanamycin selection.

2.10. Agroinfiltration

Leaves from young 4- to 6-week-old *Nicotiana tabacum* (cv Petit Havana SR1) plants were infiltrated with *A. tumefaciens* containing the appropriate plasmid at an optical density of 0.3 as described previously [34]. Leaves were incubated for 2–3 d at 25 °C in light before observation. Small sections of infiltrated leaves were placed on a microscope slide using double-sided tape and visualized without a coverslip with a 63× water immersion objective attached to a Leica TCS SP5 confocal laser scanning microscope. RFP was excited at 561 nm and detected in the 570- to 638-nm range.

3. Results

3.1. A KDEL cysteine protease, LlCYP is up-regulated in senescing L. longiflorum tepals

Using degenerate primers followed by RACE-PCR a full-length open reading frame of a *Lilium longiflorum* KDEL cysteine protease (*LlCYP*) was obtained from outer tepal cDNA. The predicted open reading frame of *LlCYP* encodes a 356-amino acid papain-like cysteine-protease, which showed 68-74% homology with senescence related proteases (Fig. 1A; Supplementary Fig. 2). Catalytic residues cys-154 and his-289 and several other characteristic amino acids are conserved, including Gln-148, which helps in forming the oxyanion hole, and asn-310, which orients the imidazolium ring of his-

289. The so-called "ERFNIN motif" and the "GCNGG motif", characteristic of cathepsin L and H like cys-proteases [35] are also present. Notably, LlCYP protein possesses a KDEL motif at the C-terminus, which acts as an ER-retention/retrieval signal and identifies LlCYP as a member of the plant-unique group of papain-like KDEL proteases (Fig. 1B).

The use of the programs SignalP and TargetP [28] and the comparison with similar senescence-related KDEL-proteases [36] allowed a prediction of the putative cleavage sites LlCYP has a N-terminal signal peptide (SP) and a pro-domain (PRO). The signal peptide is probably cleaved between amino acids 25 and 26, and the pro-peptide between amino acids 129 and 130. Thus the predicted MW of unprocessed LlCYP, pro-protein and mature form are 39.7, 37.3 and 24.4 KDa, respectively

Quantitative real time-PCR was used to investigate the expression pattern of *LlCYP* during tepal senescence. *LlCYP* transcripts were detected at eight stages of flower development from D-2 which corresponds to a closed bud, through D3, open flower, to D10, a fully senescent flower (Fig. 2A). *LlCYP* mRNA levels were low during bud development to full bloom but then increased in early senescence reaching a maximum in later senescence at D7 where transcript level was almost 13 times higher than at D-2. *LlCYP* was preferentially expressed in tepals as very low levels of expression were detected in the ovary, style and stamen. In leaves, expression increased slightly in early leaf senescence but decreased again in later senescence (yellow leaves) (Fig. 2B).

3.2. Transformed Arabidopsis expressing LlCYP without KDEL display early onset of senescence

Two constructs expressing *LlCYP* fused to RFP and driven by the 35S promoter were used for stable transformation of Arabidopsis: *35S::sppro::RFP::CYP* (C3) and *35S::sppro::RFP::CYPΔKDEL* (C4) (Fig. 3A). Expression of the transgenic construct was verified by RT-PCR (Supplementary Fig. 3).

During the early stages of growth, transgenic plants were morphologically indistinguishable from wild-type plants. However, by approximately 4 weeks of growth, plants expressing LlCYP lacking the terminal KDEL (C4) grew much less vigorously than both the wild type and plants over-expressing the full LlCYP (C3) (Fig. 3B). The first 5/6 rosette leaves of C4 plants started to show yellowing and an early senescence phenotype, while C3 plants were indistinguishable from the non-transgenic counterparts. As C4 plants continued growing, only the newly emerged leaves remained

green (Fig. 3C). After 8 weeks C4 plants showed a very small rosette compared to wild type, which corresponded to a reduced fresh weight of approximately 1/10 (Fig. 3E). Both C3 and C4 lines displayed a significant delay in bolting and flowering (Fig. 3D) while no significant differences were observed between wild-type and transgenic plants in terms of number of leaves (Fig. 3E and 3C).

3.3. LlCYP is recognised by a KDEL protease-specific antibody and is processed in senescing petals

LlCYP was expressed in *E. coli* and an antibody raised against the SlCypEP KDEL-tailed protease from tomato anthers [23] was used for immunological analysis. A protein of about 45 KDa, was recognised in agreement with the predicted size of the un-processed LlCYP protein (Fig 4A). In *L. longiflorum* tepal extracts, three bands were detected at each stage of development. The sizes of these bands correspond to those of the LlCYP pro-protein (about 45 KDa), a putative processing intermediate (about 43 KDa) and mature LlCYP (about 35 KDa) (Fig. 4B). The abundance of the 45, 43, and 35 KDa proteins peaked at stages D3 and D4 (open flower), falling back slightly at stages D5 and D7 (early senescence) and increasing sharply again in late senescence at D10. At stage D4 a protein of about 40 KDa was detectable (asterisk) which may represent a further processing intermediate.

3.4. LlCYP localises to the ER in young tissues but increasingly reaches the vacuole in senescent petals

To examine the intracellular localisation of *LlCYP*, constructs expressing the full ORF fused to RFP and driven by the 35S promoter were infiltrated into young tobacco leaves (Fig. 5). Confocal images show localisation to the ER (as indicated by the strong labelling of the nuclear envelope in C) in the presence of the terminal KDEL ER-retention signal (Fig. 5A and C). When the KDEL sequence was deleted, fluorescence was still seen in the ER but also detected in the lumen of the vacuole (Fig. 5B, asterisks, and D). A similar pattern of expression was seen in leaves from Arabidopsis transgenic lines transformed with constructs C3 and C4 (Fig 5E-H). For lines carrying the C4 construct, the protein was also detected in the apoplast (Fig. 4H, arrowheads) and vacuole. This profile is compatible with a protein which is being released slowly from the ER towards secretion, but with a pool which is still being directed to the vacuole.

The localisation of LlCYP was further examined by electron microscopy and using the SlCysEP antibody for immunogold staining. In tepals from stage D5 small electron-opaque structures appeared within the vacuole (Fig. 6A, indicated by arrows). Immunogold labelling with anti SlCysEP resulted in numerous gold particles being detected on these intravacuolar structures (Fig. 6B and C). A control experiment with pre-immune serum showed no gold labelling (data not shown). Similar structures and immunogold labelling were not detected in tissues at stage D0 (opening flowers) or from flowers at full bloom (stage D3) (data not shown).

To further assess the re-localisation of LlCYP during senescence, RFP signal was monitored in Arabidopsis transgenic lines expressing the C3 construct in young and old leaves (Fig. 6D and E). A stronger signal is seen in the vacuole in older leaves compared to young leaves.

4. Discussion

The KDEL cysteine protease identified here from *Lilium longiflorum* senescent petals shows closest homology to a similar protein (PRT5) identified in *Sandersonia aurantica* senescent petals [9] and close homology to proteins (SEN11 and SEN102) identified in *Hemerocallis* [14] (Fig. 1). Like both *PRT5* and *SEN11*, *LlCYP* is expressed at very low levels during bud opening and expression only increases once flowers are mature, with levels rising as the tepals enter senescence. Expression of these genes is also low or undetectable in other tissues and seems to decline with leaf senescence. As was the case for PRT5, LlCYP also cross-reacted with antibodies raised to KDEL cysteine proteases identified from other tissues and species and showed a similar banding pattern [9]. The largest protein band on western blots declined with the progression of senescence while lower molecular weight cross-reacting proteins increased in abundance suggesting processing of KDEL cysteine proteases into a mature and presumably active form during petal senescence. Bands of intermediate size were also detected and likely to be processing intermediates as also found in other systems [23,24]. Thus it seems that the most important function of these cysteine proteases is likely to be during petal senescence.

Expression of LlCYP and LlCYPΔKDEL in Arabidopsis confirmed the importance of the KDEL retention signal. Expression of the protein without its retention signal resulted in small plants showing premature senescence and death. This is very similar to what happens with over-expression of *Vigna mungo* SH-EP lacking its KDEL (SH-

EPΔKDEL). In contrast expression of the intact *Vigna mungo* cysteine protease had very little phenotypic effect [24]. Interestingly over-expression of both intact LlCYP and LlCYPΔKDEL delayed both bolting and flowering compared to WT but LlCYPΔKDEL did not affect the number of leaves produced. Thus the premature induction of senescence and death is not due to premature flowering.

Localisation of LlCYP and LlCYPΔKDEL constructs infiltrated into tobacco leaves and in the transgenic plants confirmed that removal of the KDEL resulted in dispersal of the RFP signal fused to the LlCYP protein into the vacuole. Thus the induction of early senescence and death in transgenic plants expressing the LlCYPΔKDEL protein is consistent with a premature activation of LlCYP activity in the vacuole or apoplastic space as concluded by Okamoto *et al.* [24] for the *Vigna mungo* SH-EP protein.

Both in *Vigna mungo*, and when expressed in transgenic Arabidopsis, SH-EP accumulated in 200-700 nm vesicles known as KDEL vesicles [24]. No such vesicles were seen either in *Lilium longiflorum* petals or in leaves from the transgenic Arabidopsis lines expressing LlCYP or LlCYPΔKDEL; nor were ricinosomes seen in the *L. longiflorum* petals at any stage of development or senescence. However in senescent *L. longiflorum* petals, and in transgenic Arabidopsis, LlCYP was seen inside the vacuole in senescent tissues. This is consistent with the vacuolar localisation of SH-EP in germinating *V. mungo* seedlings [24].

The absence of cytosolic vesicles associated with LlCYP suggests a difference in the transport mechanism of this cysteine protease to the nucleus. KVs bud off from the ER and appear to transport SH-EP to the vacuole by a Golgi-independent mechanism [37]. Ricinosomes do not deliver their cargo to the vacuole but directly into an acidified cytoplasm [38]. Since the report of KDEL proteins associated with ricinosomes in *Hemerocallis* petals [16] it was assumed that KDEL proteins associated with petal senescence would follow this route. Their main site of function would then be in the acidified cytoplasm after tonoplast rupture and thus very late in the cell death process. However since LlCYP appears to be translocated from the ER to the vacuole presumably via a Golgi dependent or a Golgi-independent route [39] this strongly indicates a localisation of LlCYP within the vacuole before tonoplast rupture perhaps with a role in the maturation of other lytic enzymes, as well as perhaps a role later once released by vacuolar collapse into the cytoplasm.

Acknowledgments

The authors would like to thank Dr Ant Hann (Cardiff University) and Dr Tony Stead (Royal Holloway University of London) for their assistance and advice with the electron microscopy and Steve Hope (Cardiff University) for sequencing. We also thank Prof John Greenwood (University of Guelph) for his kind donation of the tomato cysteine protease antibody and his very helpful advice.

Supplementary material

Table S1: list of primers used for PCR

Figure S1. DNA sequence of constructs used to transform Arabidopsis and for infiltration of tobacco leaves

Figure S2 Alignment of LlCYP amino acid sequence with other cysteine proteases performed using Clustal W multiple alignment. Accession numbers are as in Fig 1A.

Figure S3: Analysis of relative expression level of the constructs expressing LlCYP fused to RFP in the transgenic Arabidopsis plants. Real-time PCR was performed by using primers amplifying a fragment of the RFP transcript (primers 6 and 10, see primer list). Transcript levels were normalized using ubiquitin expression as internal standard (Ubiquitin10, At4G05320). Data are means ± SD (n = 5).

5. References

[1] H.J. Rogers, Programmed cell death in floral organs: how and why do flowers die? Ann. Bot. 97 (2006) 309-315.

[2] W.G. van Doorn, E.J. Woltering, Physiology and molecular biology of petal senescence, J. Exp. Bot. 59 (2008) 453–480.

[3] W.G. van Doorn, E.P. Beers, J.L. Dangl, V.E. Franklin-Tong, P. Gallois, I. Hara-Nishimura, A.M. Jones, M. Kawai-Yamada, E. Lam, J. Mundy, L.A.J. Mur, M. Petersen, A. Smertenko, M. Taliansky, F. Van Breusegem, T. Wolpert, E. Woltering, B. Zhivotovsky, P. Bozhkov, Morphological classification of plant cell deaths, Cell Death Diff. 18 (2011) 1241–1246.

[4] M.T. Smith, Y. Saks, J. van Staden, Ultrastructural changes in the petal of senescing flowers of Dianthus caryophyllus L., Ann. Bot. 69 (1992) 277-285.

[5] W.G. van Doorn, P.A. Balk, A.M. van Houwelingen, F.A. Hoeberichts, R.D. Hall, O. Vorst, C. van der Schoot, M.F. van Wordragen, Gene expression during anthesis and senescence in Iris flowers, Plant Mol. Biol. 53 (2003) 845–863.

[6] R. Battelli, L. Lombardi, H.J. Rogers, P. Picciarelli, R. Lorenzi, N. Ceccarelli, Changes in ultrastructure, protease and caspase-like activities during flower senescence in Lilium longiflorum, Plant Sci. 180 (2011) 716–725.

[7] C. Wagstaff, M.K. Leverentz, G. Griffiths, B. Thomas, U. Chanasut, A.D. Stead, H.J. Rogers, Cysteine protease gene expression and proteolytic activity during senescence of Alstroemeria petals, J. Exp. Bot. 53 (2002) 233-240.

[8] P. Stephenson, B. Rubinstein, Characterization of proteolytic activity during senescence in daylilies, Physiol. Plant.104 (1998) 463–473.

[9] J.R. Eason, D.J. Ryan, T.T. Pinckney, E.M. O'Donoghue, Programmed cell death during flower senescence: isolation and characterization of cysteine proteinases from Sandersonia aurantiaca, Funct. Plant Biol. 29 (2002) 1055–1064.

[10] C. Wagstaff, I. Bramke, E. Breeze, S. Thornber, L. Harrison, B. Thomas, V. Buchanan-Wollaston, A.D. Stead, H. J Rogers, A unique group of genes respond to cold drought stress in cut Alstroemeria flowers whereas ambient drought stress accelerates developmental expression patterns, J. Exp. Bot. 61 (2010) 2905-2921.

[11] A.M Price, D.F. Aros Orellana, R. Stevens, R. Acock, V. Buchanan-Wollaston, A.D. Stead, H.J. Rogers, A comparison of leaf and petal senescence in wallflowers (Erysimum linifolium) reveals common and distinct patterns of gene expression and physiology, Plant Physiol. 147 (2008) 1898-1912.

[12] M.L. Jones, G.S. Chaffin, J.R. Eason, D.G. Clark, Ethylene-sensitivity regulates proteolytic activity and cysteine protease gene expression in petunia corollas, J. Exp. Bot. 56 (2005) 2733-2744.

[13] E.P. Beers, A.M. Jones, A.W. Dickermann, The S8 serine, C1A cysteine and A1 aspartic protease families in Arabidopsis, Phytochemistry 65 (2004) 43-58.

[14] F.D. Guerrero, M. De la Calle, M.S. Reid, V. Valpuesta, Analysis of the expression of two thiolprotease genes from daylily (Hemerocallis spp.) during flower senescence, Plant Mol. Biol. 15 (1998) 11-26.

[15] M. Helm, M. Schmid, G. Hierl, K. Terneus, L. Tan, F. Lottspeich, M.J. Kieliszewski, C. Gietl, KDEL-Tailed cysteine endopeptidases involved in programmed cell death, intercalation of new cells, and dismantling of extensin scaffold, Am. J. Bot. 95 (2008) 1049–1062.

[16] M. Schmid, D. Simpson, C. Gietl, Programmed cell death in castor bean endosperm is associated with the accumulation and release of a cysteine endopeptidase from ricinosomes, PNAS 96 (1999) 14159–14164.

[17] V. Valpuesta, N.E. Lange, C. Guerrero, M.S. Reid, Up-regulation of a cysteine protease accompanies the ethylene-insensitive senescence of daylily (Hemerocallis) flowers, Plant Mol. Biol. 28 (1995) 575–582.

[18] L. Lerslerwong, S. Ketsa, W.G. van Doorn, Protein degradation and peptidase activity during petal senescence in Dendrobium cv. Khao Sanan, Postharv. Biol. Tech. 52 (2009) 84–90.

[19] H.H. Mollenhauer, C. Totten, Studies on seeds: Microbodies, glyoxysomes, and ricinosomes of castor bean endosperm, Plant Physiol. 46 (1970) 794–799.

[20] E. L. Vigil, Cytochemical and developmental changes in microbodies (glyoxysomes) and related organelles of castor bean J. Cell Biol. 46 (1970), 435–454.

[21] M. Schmid, D.J. Simpson, H. Sarioglu, F. Lottspeich, C. Gietl, The ricinosomes of senescing plant tissue bud from the endoplasmic reticulum, PNAS 98 (2001) 5353–5358.

[22] J.S. Greenwood, M. Helm, C. Gietl, Ricinosomes and endosperm transfer cell structure in programmed cell death of the nucellus during Ricinus seed development, PNAS 102 (2005) 2238–2243.

[23] A. Senatore, C.P. Trobacher, J.S. Greenwood, Ricinosomes predict programmed cell death leading to anther dehiscence in tomato. Plant Physiol. 149 (2009) 775–790.

[24] T. Okamoto, T. Shimada, I. Hara-Nishimura, M. Nishimura, T. Minamikawa, C-terminal KDEL sequence of a KDEL-tailed cysteine proteinase (sulfhydryl-endopeptidase) is involved in formation of KDEL vesicle and in efficient vacuolar transport of sulfhydryl-endopeptidase, Plant Physiol. 132 (2003) 1892-1900.

[25] E.L. Dempster, K.V. Pryor, D. Francis, J.E. Young, H.J. Rogers, Rapid DNA extraction from ferns for PCR-based analyses, Biotechniques 27 (1999) 66–68.

[26] T.A. Hall, BioEdit: a user-friendly biological sequence alignment editor and analysis program for Windows 95/98/NT. Nuc. Ac. Symp. Ser. 41 (1999) 95-98.

[27] K. Tamura, J. Dudley, M. Nei, S. Kumar, MEGA4: Molecular Evolutionary Genetics Analysis (MEGA) software version 4.0. Mol. Biol. Evol. 24 (2007) 1596-1599.

[28] O. Emanuelsson, S. Brunak, G. von Heijne, H. Nielsen, Locating proteins in the cell using TargetP, SignalP, and related tools, Nature Prot. 2, (2007) 953-971.

[29] S. Rozen, H.J. Skaletsky, Primer3 on the WWW for general users and for biologist programmers. In: Krawetz S, Misener S eds. Bioinformatics Methods and Protocols: Methods in Molecular Biology. Humana Press, Totowa, NJ, (2000) 365-386.

[30] K.J. Livak, T.D. Schmittgen, Analysis of relative gene expression data using real time quantitative PCR and the $2^{-\Delta\Delta CT}$ method. Methods 25 (2001), 402-408.

[31] E.S. Reynolds, The use of lead citrate at high pH as an electron-opaque stain in electron microscopy, J. Cell Biol. 17 (1963) 208–212.

[32] P.R. Hunter, C.P. Craddock, S. Di Benedetto, L.M. Roberts, L. Frigerio, Fluorescent reporter proteins for the tonoplast and the vacuolar lumen identify a single vacuolar compartment in Arabidopsis cells, Plant Physiol. 145 (2007) 1371–1382.

[33] S.J. Clough, A.F. Bent, Floral dip: a simplified method for *Agrobacterium*-mediated transformation of *Arabidopsis thaliana*, Plant J. 16 (1998) 735–743.

[34] H. Batoko, H.Q. Zheng, C. Hawes, I. Moore, A Rab1 GTPase is required for transport between the endoplasmic reticulum and Golgi apparatus and for normal Golgi movement in plants, Plant Cell 12 (2000) 2201-2217.

[35] N.D. Rawlings, A.J. Barrett, Families of serine peptidases, Meth. Enzym. 244 (1994) 19-61.

[36] M. Schmid, D. Simpson, F. Kalousek, C. Gietl C, A cysteine endopeptidase with a C-terminal KDEL motif isolated from castor bean endosperm is a marker enzyme for the ricinosome, a putative lytic compartment. Planta 206 (1998) 466–475.

[37] K. Toyooka, T. Okamoto, T. Minamikawa, Mass transport of proform of a KDEL-tailed cysteine proteinase (SH-EP) to protein storage vacuoles by endoplasmic reticulum–derived vesicle is involved in protein mobilization in germinating seeds, J. Cell Biol. 148 (2000) 453-464.

[38] G. Hierl, U. Vothknecht, C. Gietl, Programmed cell death in *Ricinus* and *Arabidopsis*: the function of KDEL cysteine peptidases in development. Physiol. Plantar. 145 (2012) 103–113.

[39] L. Xiang, E. Etxeberria, W. Van den Ende, Vacuolar protein sorting mechanisms in plants, FEBS J. 280 (2013) 979–993.

[40] N. Saitou, M. Nei, The neighbor-joining method: A new method for reconstructing phylogenetic trees, Mol. Biol. Evol. 4 (1987) 406-425.

[41] J. Felsenstein, Confidence limits on phylogenies: An approach using the bootstrap, Evolution 39 (1985) 783-791.

[42] E. Zuckerkandl, L. Pauling L, Evolutionary divergence and convergence in proteins, in: Evolving Genes and Proteins, V. Bryson and H.J. Vogel eds. Academic Press, New York (1965) 97-166.

FIGURE LEGENDS

Fig. 1. Comparison of *LlCYP* open reading frame with other cysteine proteases. (A) Phylogenetic tree. The evolutionary history was inferred using the Neighbor-Joining method [40]. The optimal tree with the sum of branch length = 2.64260549 is shown. The percentage of replicate trees in which the associated taxa clustered together in the bootstrap test (1000 replicates) is shown next to the branches [41]. The tree is drawn to scale, with branch lengths in the same units as those of the evolutionary distances used

to infer the phylogenetic tree. The evolutionary distances were computed using the Poisson correction method [42] and are in the units of the number of amino acid substitutions per site. All positions containing gaps and missing data were eliminated from the dataset (Complete deletion option). There were a total of 329 positions in the final dataset. Phylogenetic analyses were conducted in MEGA4 [27] and databsae accession numbers are shown next to each genus and gene name on the tree. (B) Alignment of the most closely related cysteine protease to LlCYP. The "ERFNIN motif" within the pro-sequence and amino acids belonging to the catalytic pocket (Cys-154 and His 289) or otherwise important for catalysis (Gln-148 and Asn-310) are in red, Cysteine residues involved in disulfide bridges are in blue and the C-terminal KDEL is in green. The arrows represent the predicted putative cleavage sites.

Fig. 2. Expression of *LlCYP* gene. (A) Relative expression of *LlCYP* gene throughout development and senescence from stage D-2 (closed bud) to stage D10 (full senescence). (B) *LlCYP* transcript levels in different flower organs and in leaves.
Relative expression levels are shown as fold change values (1 = D-2 tepals). Transcript levels were normalized to 18S rRNA, used as internal standard. Data are means ± SD (n = 3).

Fig. 3. Aerial phenotype of LlCYP transgenic lines. (A) Schematic representation of the constructs used for plant transformation. In construct C3, RFP is sandwiched between the LlCYP prepro-sequence and the rest of the open reading frame, all inserted in the pK7WG2 vector. C4 is the same construct but lacking the terminal KDEL.
(B) Phenotype of 6-week-old transgenic Arabidopsis plants grown on soil (WT, C3 and C4).
(C) Rosette leaves from 6-week-old plants (WT, C3 and C4) arranged in order (left to right) from the youngest to the oldest. Bar = 10 mm.
(D) Bolting and flowering time, (E, F) whole rosette fresh weight and total leaves number in C3 and C4 transgenic lines compared to WT plants at 8 weeks (±SE, $n = 30$). Asterisks indicate significant difference to WT at $P < 0.05$ (*) or $P < 0.01$ (**). Data are representative of three independent experiments.

Fig. 4. LlCYP protein in senescing petals. (A) Western blot using SlCysEP antibody showing recognition of a 45kDa band in crude extracts of *in vitro* expressed LlCYP (negative control is an uninduced culture, positive control is SlCysEP purified protein).

(B) Western blot of *L. longiflorum* tepal protein extracts from outer tepals at different stages of development and senescence. Blots were incubated with a primary antibody raised against SlCysEP (below the western blot is a Coomassie stained gel as loading control). The 43 kDa and 40 kDa (denoted by asterisk) bands are putative processing intermediates.

Fig. 5. Subcellular localization of of LlCYP-RFP constructs.

(A) and (C): confocal images of tobacco leaves infiltrated with *Agrobacteria* harbouring construct C3; (B and D): tobacco leaves infiltrated with construct (C4). Nuclear envelope is indicated by NE; (E and G): transgenic Arabidopsis seedlings over-expressing the C3 construct; (F and H): transgenic Arabidopsis over-expressing the C4 construct. White arrowheads indicate presence of the RFP signal in the apoplastic space; asterisks indicate fluorescence in the vacuolar lumen. Scale bars: 20 μm (A and C); 5 μm (B and D); 10 μm (E-H).

Fig. 6. Subcellular localization of LlCYP in the tepals of L. longiflorum.

Transmission electron micrographs of cells of *L. longiflorum* tepals at stage D5. Electron dense structures appear within the vacuole (A) of cells at stage D5.

(B,C) Immunogold localization of LlCYP in cells of *L. longiflorum* tepals at stage D5.

(A) Magnification 2.5 K, scale bar, 3 μm; (B) Magnification 40 K, scale bar, 100 nm; (C) Magnification 50 K, scale bar, 100 nm; (D) and (E) confocal images of transgenic Arabidopsis leaves expressing the C3 construct: (D) young leaves, (E) old leaves; Scale bars, 10 μm.

Figure(s)

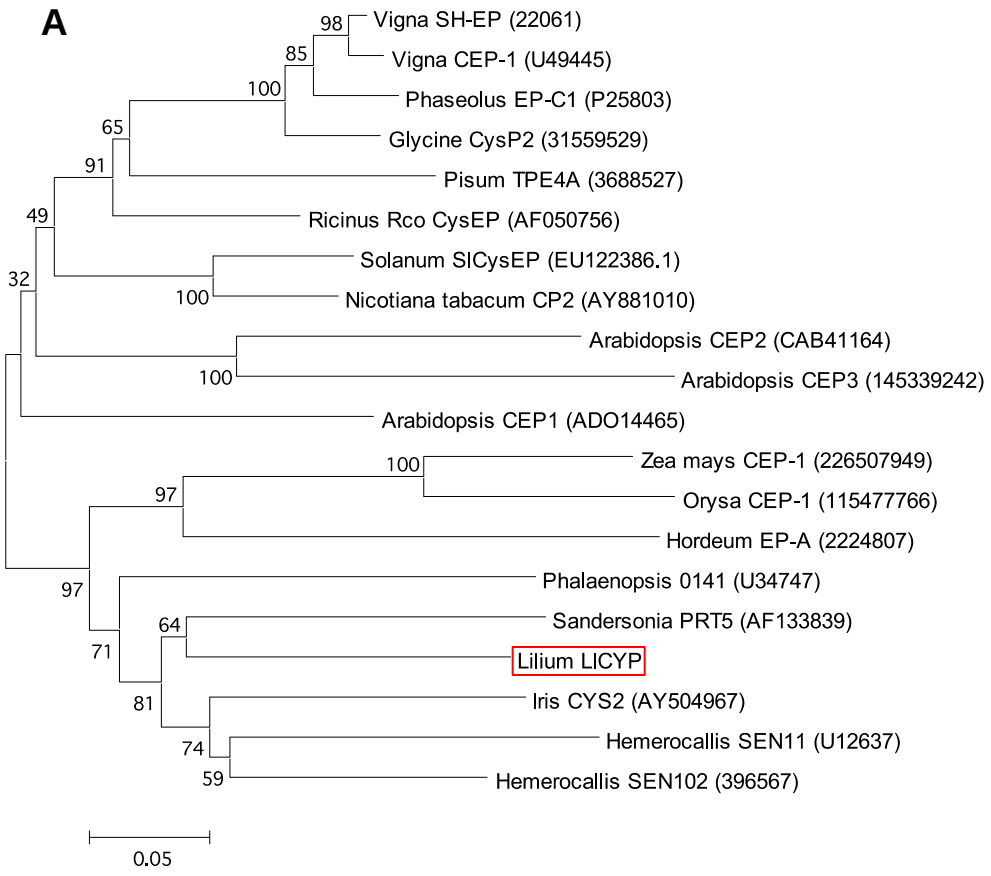

B

Figure 1

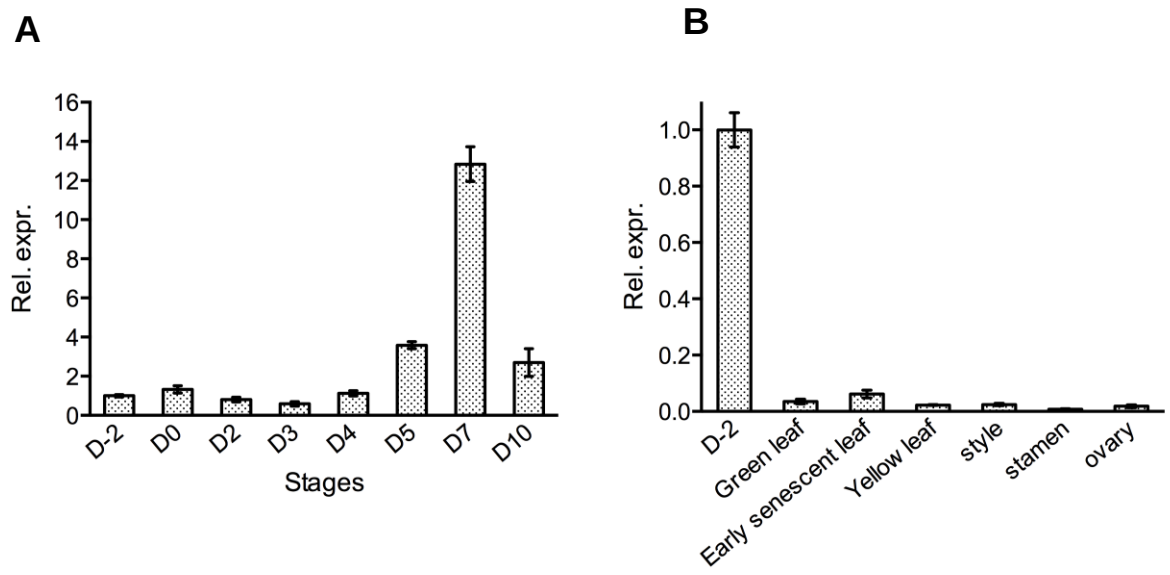
A
Rel. expr.
16
14
12
10
8
6
4
2
0
D-2
D0
D2
D3
D4
D5
D7
D10
Stages
B
Rel. expr.
1.0
0.8
0.6
0.4
0.2
0.0
D-2
Green leaf
Early senescent leaf
Yellow leaf
style
stamen
ovary

Figure 2

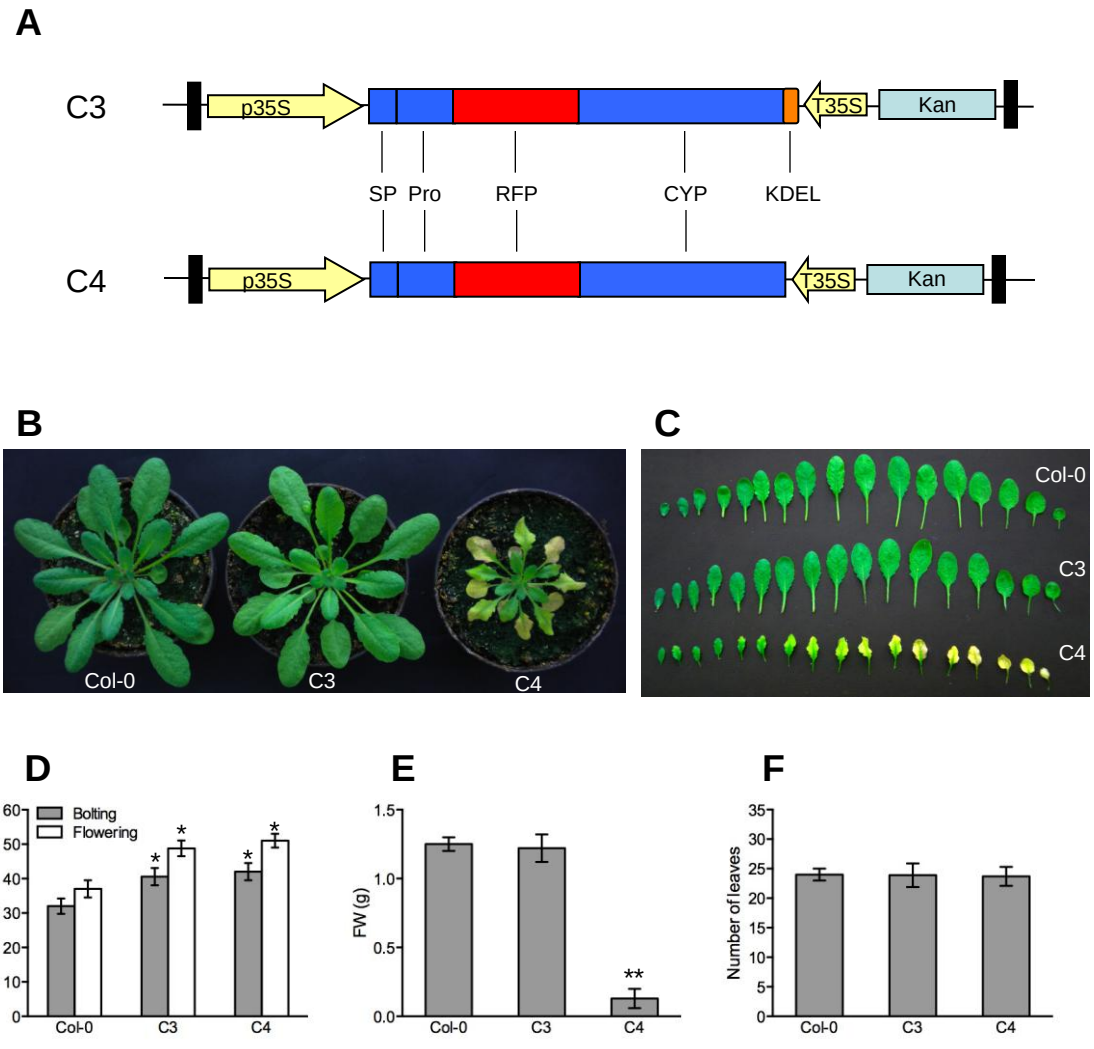
A
C3
p35S
T35S
Kan
SP
Pro
RFP
CYP
KDEL
C4
p35S
T35S
Kan
B
Col-0
C3
C4
C
Col-0
C3
C4
D
Bolting
Flowering
Days
Col-0
C3
C4
E
FW (g)
Col-0
C3
C4
F
Number of leaves
Col-0
C3
C4

Figure 3

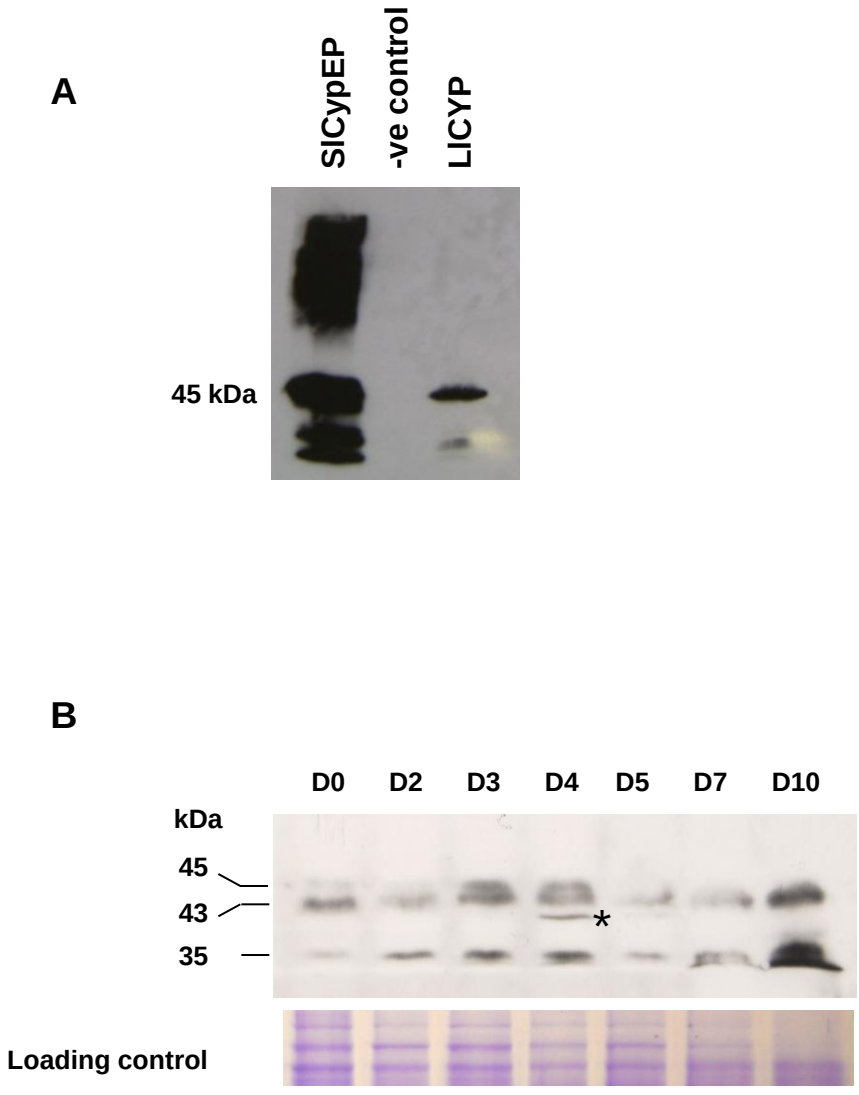
A
SlCypEP
-ve control
LlCYP
45 kDa
B
D0
D2
D3
D4
D5
D7
D10
kDa
45
43
35
*
Loading control

Figure 4

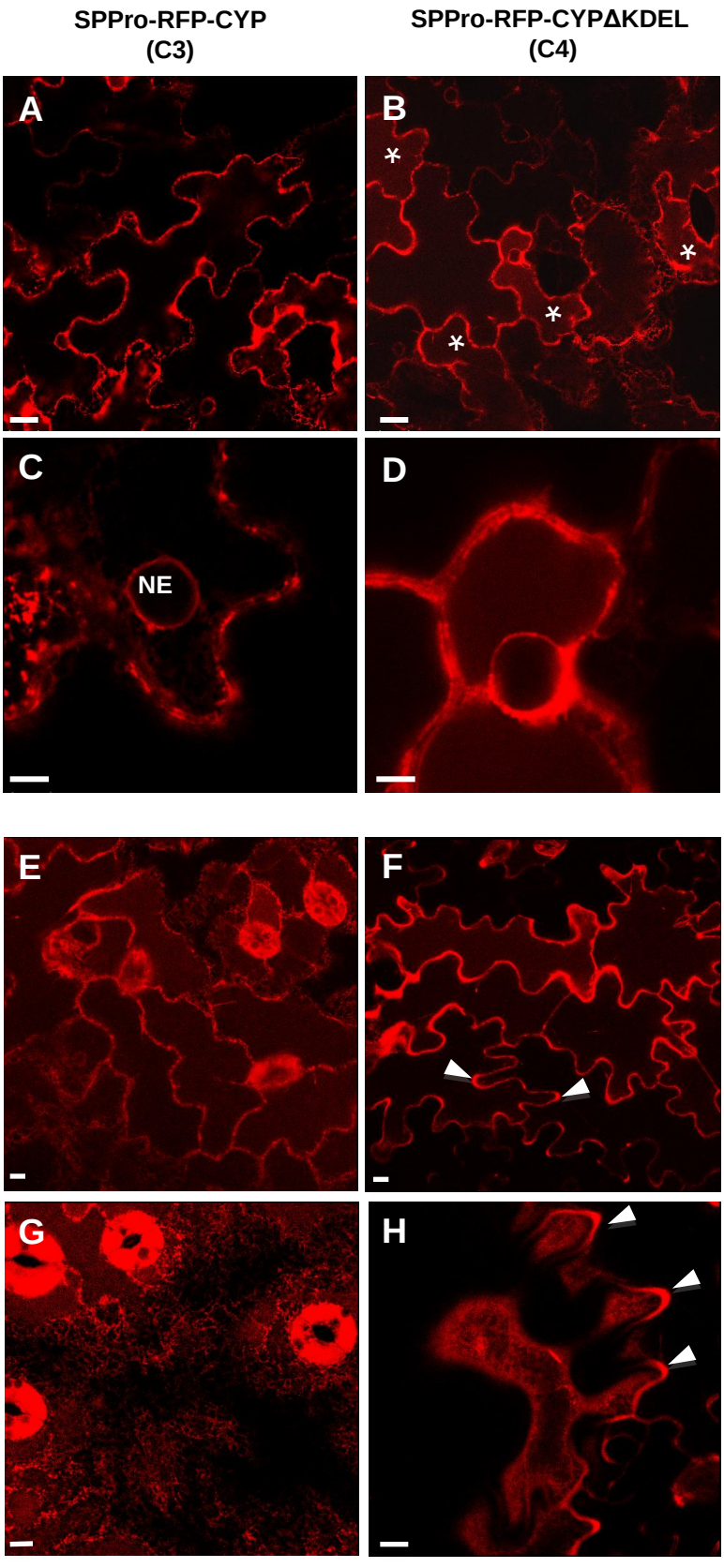

Tobacco infiltrations

Arabidopsis transgenics

Figure 5

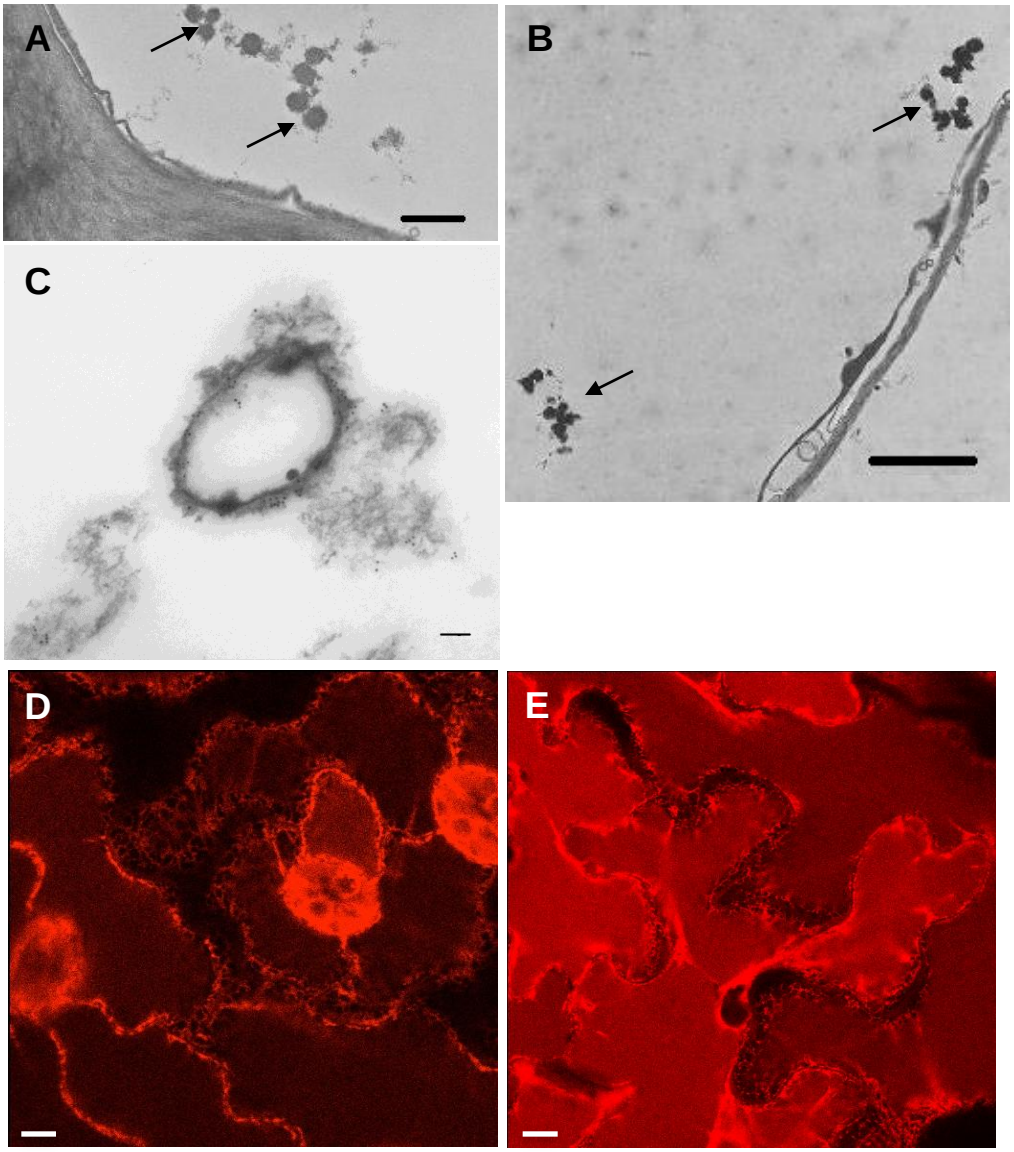

Figure 6

Ecomponent(s)

Click here to download Ecomponent(s): Revised Supplementary Tables and Figures 170913.ppt